



ESJ Natural/Life/Medical Sciences

Contribution of Aeromagnetic Data to the Structural Discontinuities Identification of Black Volta Catchment Aquifer System in Côte d'Ivoire

Armel Kouadio Kouame

Laboratory of Soil, Water and Geomaterials Sciences, Training and Research Unit of Earth, Sciences and Mineral Resources, University Felix Houphouët-Boigny, Abidjan, Côte d'Ivoire

Marc Youan Ta

University Research Center of Remote Sensing and Application (CURAT), Training and Research Unit of Earth Sciences and Mineral Resources, University Felix Houphouët-Boigny, Abidjan, Côte d'Ivoire

Bertrand Hounnigbo Akokponhoue

Laboratoire of Applied Hydrology, National Water Institute (INE), University of Abomey-Calavi, Cotonou, Benin

Omer Zéphir De Lasme

Department of Geosciences, Training and Research Unit, University Péléforo Gon Coulibaly, Korhogo, Côte d'Ivoire

Kouamé Loukou Nicolas

Laboratoire de Géologie, Ressources Minérales et Energétique, UFR Sciences de la Terre et des Ressources Minières (STRM), Université Félix Houphouët Boigny, Abidjan, Côte d'Ivoire

[Doi:10.19044/esj.2023.v19n30p307](https://doi.org/10.19044/esj.2023.v19n30p307)

Submitted: 23 June 2023

Accepted: 08 October 2023

Published: 31 October 2023

Copyright 2023 Author(s)

Under Creative Commons CC-BY 4.0

OPEN ACCESS

Cite As:

Kouame A.K., Ta M.Y., Akokponhoue B.H., De Lasme O.Z. & Kouamé L.N. (2023). *Contribution of Aeromagnetic Data to the Structural Discontinuities Identification of Black Volta Catchment Aquifer System in Côte d'Ivoire*. European Scientific Journal, ESJ, 19 (30), 307. <https://doi.org/10.19044/esj.2023.v19n30p307>

Abstract

This paper focuses on improving the structural knowledge of the fissured aquifers of the Black Volta catchment in Côte d'Ivoire based on the mapping of magnetic lineaments, which represent magnetic discontinuities such as magmatic body contacts or tectonic faults. Four filtering methods, pole reduction (equator), gradient (vertical and horizontal), upward extension, and

angle tilt, were applied to the residual magnetic field map to extract magnetic discontinuities while using the Oasis Montaj (Geosoft) program. Euler deconvolution coupled with the analytical signal provided, in addition to the horizontal location of the magnetic contacts, is an indication of their depths. The resulting structural map contains 458 structures, with lengths ranging from 9.03 to 66.54 km. Three directions, NW-SE, E-W and NE-SW, were detected with a predominance of the NW-SE direction. Depths estimated by Euler solutions range from 6.8 to 2847 m. This map is consistent with many faults already recognised or assumed by traditional structural studies and tectonic events affecting the Ivorian basement. These results contribute significantly to the improvement of the structural map of the Black Volta Basin in Côte d'Ivoire. In addition to the major known tectonic faults, numerous lineaments, particularly those at depth, have been highlighted by the present study.

Keywords: Aeromagnetic, Gesosoft Oasis Montaj, Euler Deconvolution, Structural Map, Filtering, Black Volta Catchment

Introduction

For a long time, aeromagnetic data has been used to support the mapping of geological structures and the faults that affect them. It also detects magnetic mineral concentrations through the measurement of magnetite in geological formations beneath the aircraft. Although these aeromagnetic surveys are widely used as a reconnaissance tool, there is growing recognition of their potential in the assessment of prospective areas given the unique information they provide (Reeves, 2005; Abbass et al., 2013). At present, hydrogeological applications of airborne geophysical methods are still few and generally concern the structural and lithological applications. They involve the identification of structures called geophysical lineaments. Geophysical lineaments (gravimetric and magnetic) are linear or curvilinear discontinuities caused by density or magnetization contrasts in rocks. These lineaments are usually associated with structural features such as faults, fractures, folding axes, and lithological contacts. Mapping by conventional methods (tracking faults on the ground and by aerial photographs, satellite images and radar) does not allow the identification of all existing lineaments. Certainly, airborne magnetic data, which allows us to see through surface layers such as sand, vegetation, and water, are a powerful tool for highlighting surface structures and deep, non-flush structures in the crust, whose hydraulic role is essential for exploring underground reservoirs. Experience has shown the value of geophysical data for lineament mapping and identification of geological structures (Khattach et al., 2004; Vanié et al., 2005; El Gout et al., 2010). This study aims to establish a fracturing map relevant to water

resources exploration in the Black Volta Basin in Côte d'Ivoire by identifying the structures buried in the subsurface. Aeromagnetic maps provide uniform geophysical coverage that is independent of topography. This makes it possible to identify deep and superficial structural discontinuities in the crust (too general, be precise) without constraints. Achieving a less evasive structural map, which can provide information on geometric characteristics by integrating surface, semi-profound and deep information, can be an indispensable tool for a better understanding of complex discontinuous environments.

Geological and Hydrogeological Framework

The study area (Figure 1) is the interface of the Black Volta transboundary basin in Côte d'Ivoire. It is located between latitudes 7°78 and 9°94N and longitudes 2°49 and 3°35W. Furthermore, it delimits a vast geographical area located in the northeast of Côte d'Ivoire. Its main river, the Black Volta (Mouhoun) River, originates in the Kong Mountains in the Dindéresso Forest Reserve, southwest of Burkina Faso. It is approximately 1,363 km long, and it drains a total area of 12,836 km² in Côte d'Ivoire. The relief is not very rugged. The highest peak, the Bondoukou Massif, reaches an altitude of 725 m. Geologically, the basin is located in the eastern compartment of the Precambrian basement called Baoulé-Mossi (Figure 1) of Paleo-Proterozoic, which is structured by the Eburnian megacycle (2400-1600 Ma). The eastern zone is covered by a complex set of geological formations. It is classified according to age and unevenly distributed in two domains: the Quaternary domain (Holocene) and the Birimian domain (Figure 1).

From a hydrogeological point of view, the conceptual model accepted in the basement zone indicates the presence of a superficial film (alterites). Accordingly, the capacitive fed is by the surface. This is followed by a fissured horizon (intermediate decompressed zone), with very high permeability forming the second aquifer level (Lachassagne et al., 2005). The third aquifer level is located in the sound bedrock, which is affected by tectonic fractures (faults). Level 2 and 3 constitute the semi-captive part of this multi-layered aquifer hosting a single water table (Ousmane, 1988).

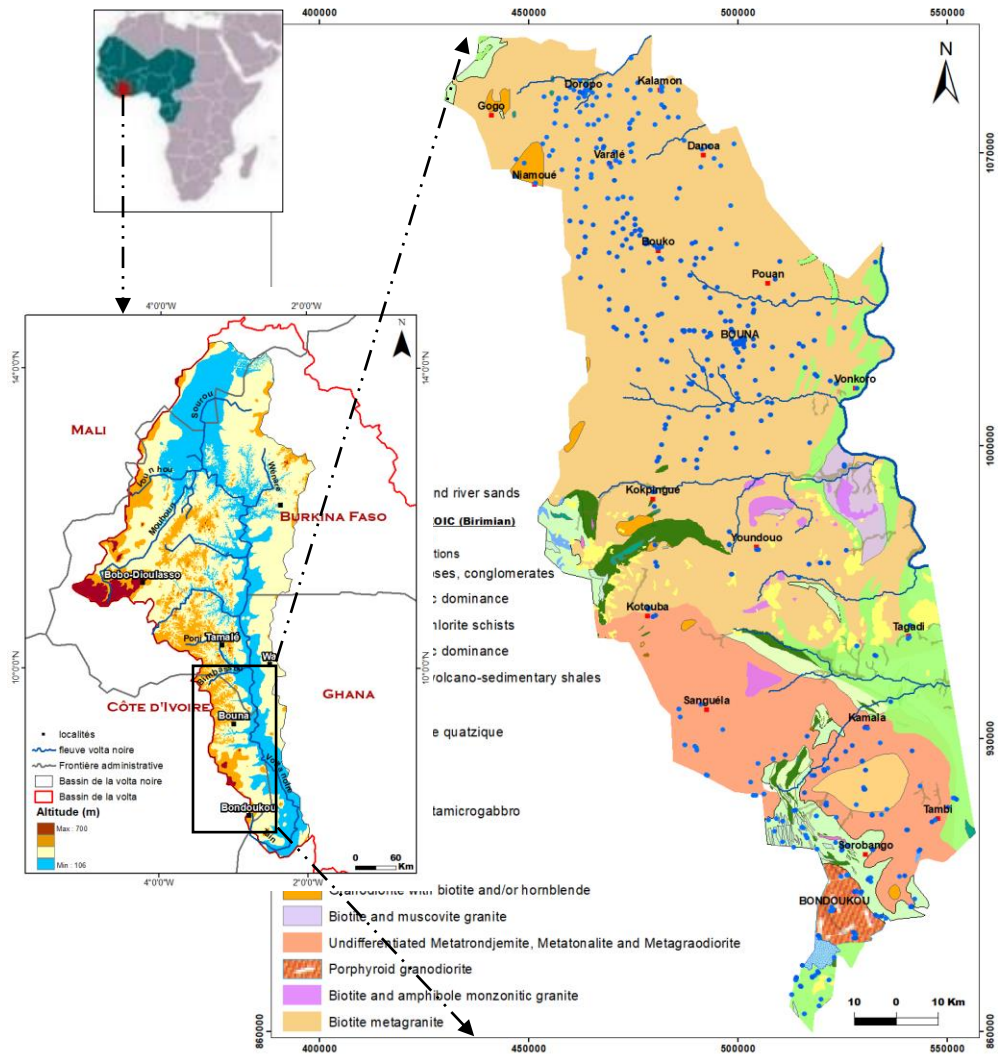


Figure 1. Geological Map of the Studied Area

Methods

Aeromagnetic Data

The data used in this study was obtained from the archives of the “Direction la Cartographie et de la Prospection Géologique (DCPG)” of the Ministry of Mines, Petroleum and Energy of Côte d'Ivoire. These data, available in the form of total magnetic field maps, were obtained by an aircraft equipped with a Geometrics G.803 proton precession magnetometer during aerial surveys. This was carried out by Kenting Earth Sciences Ltd. in 1974 and 1975 as part of a cooperative programme between the Government of Canada and the Government of the Republic of Côte d'Ivoire. However, this was done under the auspices of the Canadian International Development

Agency. The isomagnetic contours were compiled from magnetometric recordings made along the N-S oriented flight lines. The flight lines were plotted on the 1:50,000 photomosaics, and the coordinates of the turning points were determined and digitally compiled on magnetic tape. The field strengths were derived either from analogue magnetometric profiles after digital translation on tape, or from digital profiles at the nodes of a 2.5 mm square grid, according to a simulated polynomial variation of the field in the direction perpendicular to the flight lines. The grid was used as the basis for the mechanographic drawing of the original 1:50,000 map without the flight lines. For this work, two sheets covering 92% of the basin were used. The other part covers the Comoé National Park, which is of no interest for the valorisation of the results of this study.

Digital Processing Methods for Aeromagnetic Images

The aeromagnetic data provided in the form of digital maps of the total magnetic field containing isovalues curves were previously corrected (denoising, fence error, diurnal variations). The total magnetic field map was reconstructed using a GIS. The total magnetic field was subtracted from the International Geomagnetic Reference Field (IGRF), and the resulting residual magnetic field values were interpolated to a 50 m square grid. A series of treatments using optimal filters were applied to the grid to extract the maximum amount of structural information.

Reduction At The Pole (equator)

The residual magnetic field map was reduced at the pole (equator) using the parameters of the local Earth's magnetic field with declination $D = -8.2424^\circ$; inclination $I = 0.1967^\circ$, and intensity $H = 31947$ nT. It allowed the removal of the bipolarity of the magnetic anomalies, which is caused by nonvertical magnetisation directions. Thus, the magnetic anomaly values are recalculated as if they had been measured at the magnetic pole, where the magnetic field direction is vertical. In other words, it eliminated the distortions induced by the tilt of the Earth's magnetic field vector. It formed the base map for the application of the various filters and operators later on.

Vertical (dz), Horizontal (dx, dy and upward gradients)

These mathematically based operators reinforce the bodies at the origin of the anomaly by freeing them from the regional components of short and long wavelengths, thus highlighting either the location of the bodies or a lithological or structural contact between two bodies. The vertical gradient or vertical derivative of the field was applied to the reduced magnetic anomaly at the pole. The first derivative allowed better individualisation of nearby sources. The horizontal gradient along x and y allowed the magnetic effect of

geological contacts to be amplified visually by delineating the perimeter of geological bodies highlighting lithological contacts. An upward extension is carried out on the same slightly wider initial grids at a distance of 200 m.

Tilt Angle

The Tilt-angle (Miller & Singh, 1994; Verduzco et al., 2004; Salem et al., 2008) calculates the inverse tangent of the ratio, including the modulus of the horizontal partial derivatives and the vertical derivative of the magnetic field. Thus, it is written as follows:

$$\theta = \tan^{-1} \frac{\frac{\partial M}{\partial z}}{\sqrt{\left(\frac{\partial M}{\partial x}\right)^2 + \left(\frac{\partial M}{\partial y}\right)^2}} \quad (\text{Eq.1})$$

M being the grid of the magnetic field or anomaly.

The advantage of the transformation indicates that by calculating an angle, all shapes will be represented in a similar way, whether the anomalies are of low or high amplitude (Bouiflane, 2008). This operator is applied to the map of the magnetic anomaly, and it is reduced to the equator so as to discriminate the azimuth structures.

Euler Deconvolution

The Euler deconvolution method allowed the precise location of anomaly sources in the horizontal plane as well as the estimation of their depths (Keating, 1998; Asfirane-Haddadj & Galdeano, 2000). It is based on the Euler homogeneity equation (Eq.2), which relates the magnetic field and its gradient components to the location of the source, with a degree of homogeneity that a structural index (SI) can be interpreted (Thompson, 1982).

$$\frac{(x-x_0) \partial T}{\partial x} + \frac{(y-y_0) \partial T}{\partial y} + \frac{(z-z_0) \partial T}{\partial z} = N(B - T) \quad (\text{Eq.2})$$

Where (x_0, y_0, z_0) :magnetic source position ; (x, y, z) : observation point position ; T : total field strength detected at (x, y, z) ; B : regional value of total field ; N : degree of homogeneity, usually referred to as the structural index (SI). It indicates the structural index and refers to the geometry of the source and the rate of change of the field versus distance. In this work, the Euler deconvolution solutions were computed with a structural index (SI=0) to highlight the structures at depth and those affecting the cover. This aligns with the works of Vanié et al. (2005), El Gout et al. (2009), and Abderbi and Khattach (2010). Since the new method of localized Euler deconvolution supports the analytical signal, it was used instead of the standard Euler deconvolution.

The principle of the method is based on solving the equation with four unknowns: x_0, y_0, z_0 and B . All these treatments were performed using the USGS Oasis Montaj software (Geosoft).

Results

Results and Analysis of the Transformed Maps

Figure 2a shows the residual magnetic field map of the basin. It spatially spreads out the variations in the magnetic properties of the Earth's crust, thus reflecting geologically derived source structures. The reduced magnetic field map at the equator (Figure 2b) shows anomalies of size and amplitude, which varies between 31700 and 32115 nT. Two localised magnetic domains can be distinguished from north to south. The southern part, in the Gontougo region, is characterised by elongated E-W negative anomalies that are marked in the volcano-sedimentary formations. Positive anomalies oriented to NE-SW and NW-SE are more marked in the Paleo-proterozoic crustal rocks in the north. This variation in magnetic intensity reflects the heterogeneity of the underlying geological formations.

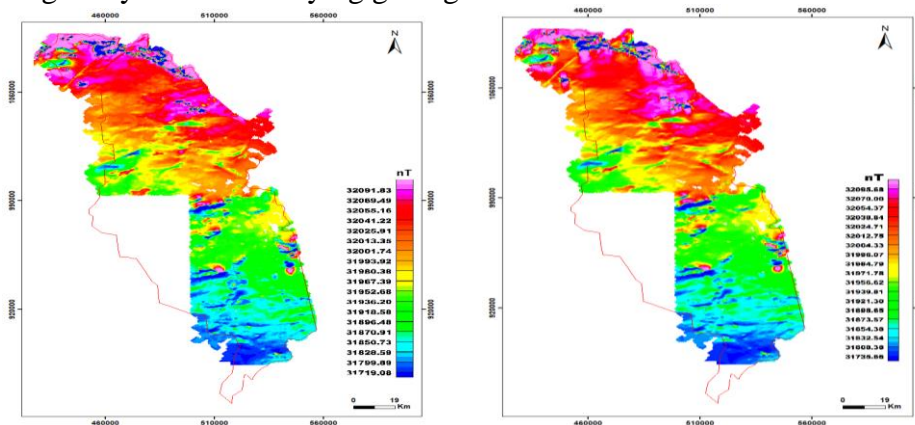


Figure 2. Transformed Maps a) Residual Magnetic Field Map, b) Map of the Reduced Field at the Equator

The first-order derivative transformed maps are shown in Figure 3. The vertical derivative (Figure 3a) highlights the surface anomalies by comparatively attenuating the long-wave (low frequency) anomalies. As the derivative order increases, the low frequency anomalies are attenuated. At the same time, the noise in the data is increased. The vertical derivative reveals anomalies that are hardly visible on the residual magnetic field maps. On these maps, the magnetic signatures are dominated by positive anomalies that describe a network of surface magnetic structures with numerous distortions. In general, they are mainly oriented to E-W and NE-SW. The horizontal derivative (Figure 3b) gives a good visualisation of these lineations. It completely eliminates the long-wave magnetic anomaly in the centre of the map. In

addition, the E-W and NE-SW lineations are better imaged and more continuous. On the upwardly extended map, the signal is smoothed out and the effects of large semi-deep structures are favoured over small surface objects. However, only the major anomalies are clearly visible. This implies that the higher the extension altitude, the smaller the amplitude of the anomalies.

Although small surface objects no longer appear on the map, the major anomalies are still clearly visible even at 60 m extension (Figure 3d).

The Tilt-angle transformation operator shows a clear structuring of the study area (Figure 3e). The magnetic lineations appear more clearly in a similar way, whether the anomalies are of low or high amplitude. In other words, while calculating an angle, all shapes are represented at the same time. The map (Figure 3e) shows the curve of the angle θ equivalent to the contact, which delimits elongated structures oriented to E-W. They are largely superimposed on the course of the hydrographic network in the basin. NW-SE and NE-SW directions are also shown. Through analytical signal, it is possible to present the magnetic anomalies stripped of any dependence on the inclination of the earth's inducing field. The anomalies that remain positive are located directly above the sources.

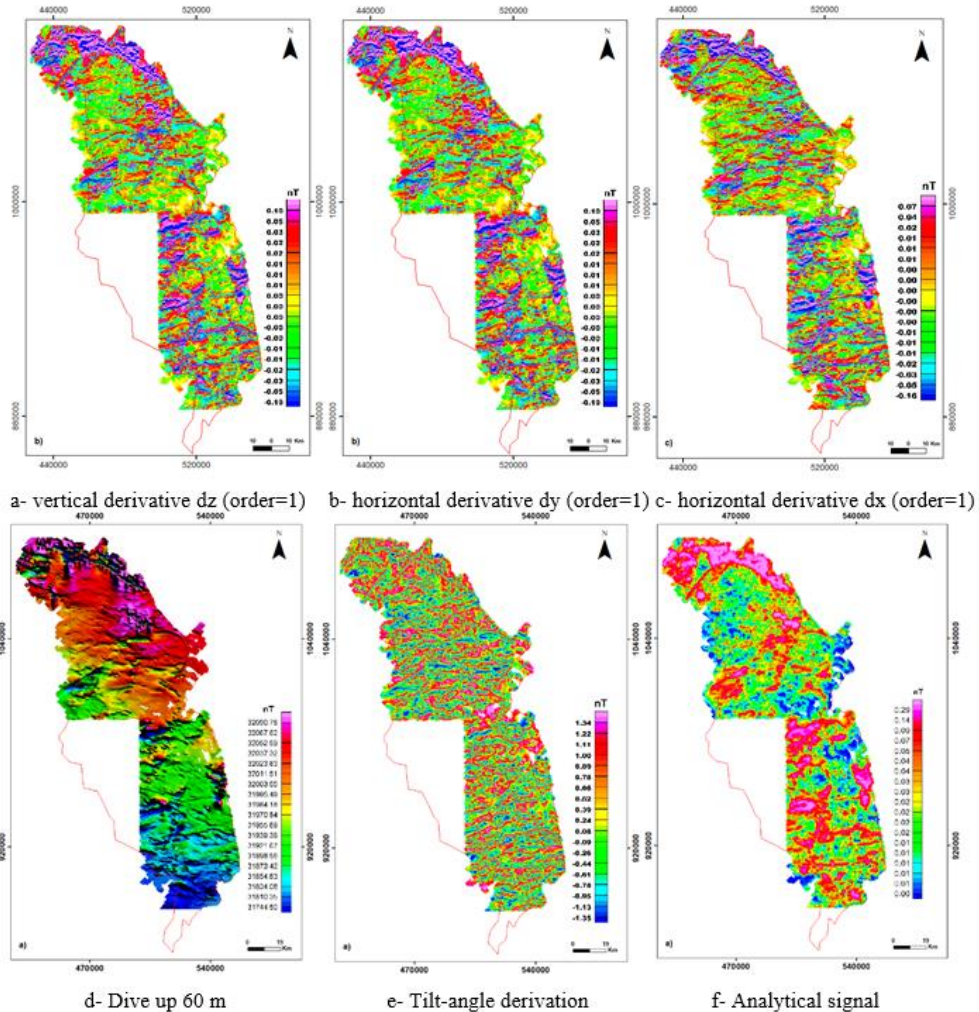


Figure 3. Magnetic Maps Transformed by Derivation (a, b, c.), Induced Field Extended Upwards to 60 m (d), Tilt-Angle Derivation (e) and Analytical Signal (f)

Structural Map

Figure 4 shows the field of major lineaments resulting from the interpretation of the transformed magnetic images. These structures correspond to two things: (i) magnetic stripes, i.e., direct observations of magnetic ridges and/or troughs associated with lithological contacts, and (ii) intersecting lineaments marked by abrupt breaks or breaks in magnetic susceptibility, with or without displacement. There are 458 lineaments with lengths ranging from 9.03 to 66.54 km and an arithmetic average of 18.33 km. The length histogram (Figure 5a) shows a strong heterogeneity in the distribution of lineament lengths. The directional rosette of the cumulative lengths (Figure 5b) indicates a predominance of the NW-SE direction

(N120-140), which is followed by the E-W (N80-90°) and NE-SW (N50-60°) directions. This distribution is confirmed by the frequency analysis.

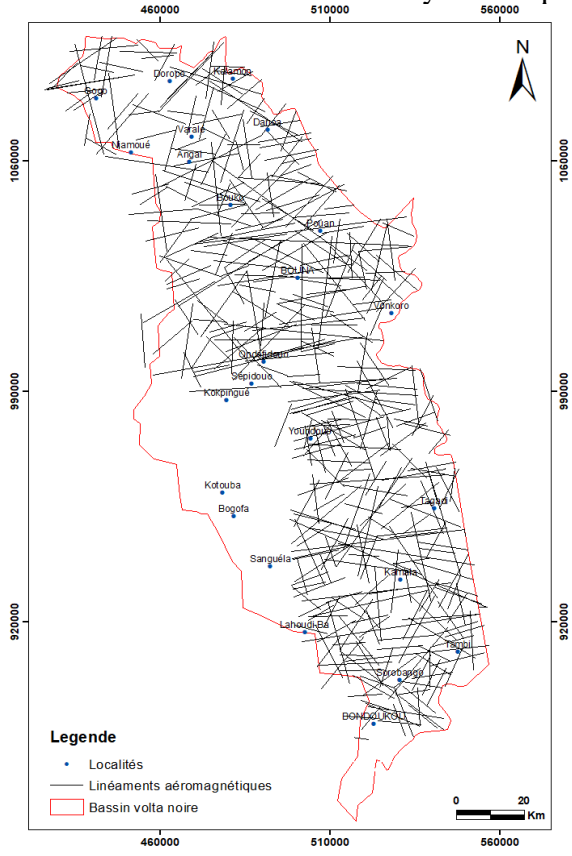


Figure 4. Structural Map of the Black Volta Catchment in Côte d'Ivoire

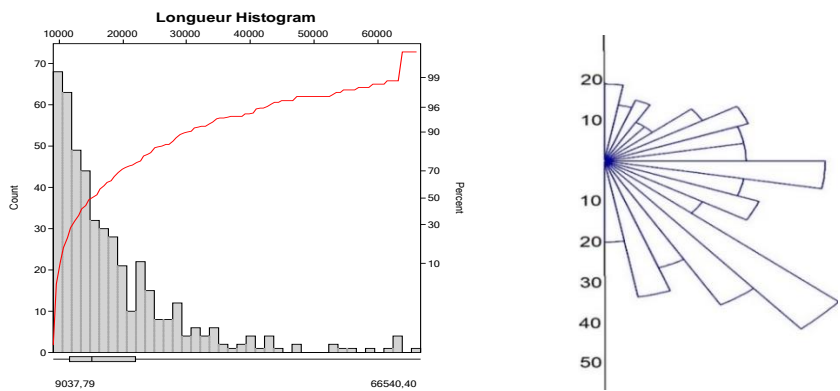


Figure 5. Geometric Parameters of Lineaments a) Lineament Length Distribution and b) Bi-directional Rosette of Cumulative Fracture Lengths from Transformed Magnetic Images

The use of Euler deconvolution coupled with the analytical signal was particularly effective in delineating the contacts and assessing their depths. Eulerian deconvolution solutions were obtained for a structural index = 0 (contact model), a window size of 10×10, and a maximum relative error of 15% on the depth. The solutions are presented in Figure 6a. The coloured dots indicate the depth of the source, and each colour is linked to one of the estimated depths, which are divided into seven (7) ranges. The estimated depths range from 6.8 to 2847 m, with a predominance of depths between 1500 and 2000 m in crystalline or metamorphic basement rocks. The superposition of these solutions on the structural cover shows the main contacts highlighted. In general, the Euler solutions show preferential N-S (N0-20°; N160-180°) and NW-SE (N110-120°) trends as illustrated in Figure 6b.

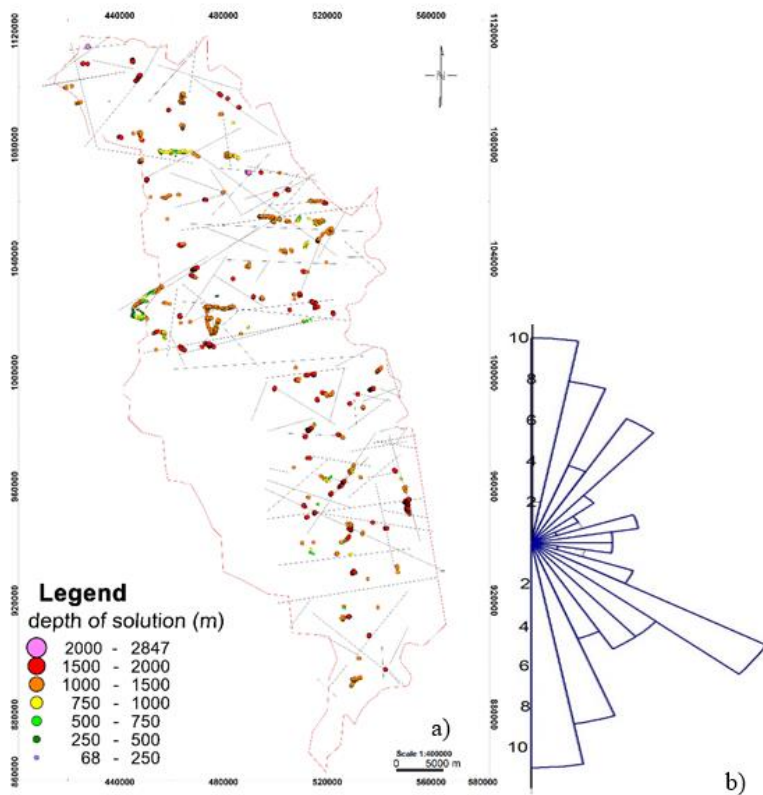


Figure 6. Euler Deconvolution Solutions of a) Aeromagnetic Data (SI=0; window=10×10 m; maximum relative error=15%); b) Directional Rosette Diagram of Deep Fractures

Discussion

This study is based on the use of aeromagnetic data in the framework of geophysics applied to structural mapping. Several filtering techniques were used to extract the maximum information on the distribution of magnetic anomalies. In geology, these methods are known either to map magnetic anomalies that may be induced by crystalline or metamorphic basement rocks or to detect linear anomalies (responses) that are dependent on tectonic and lithological contacts (Grauch et al., 2006). The methods applied in this study have a common approach, which determines the horizontal and/or depth locations of magnetic contacts. Gradients (dx, dy, and dz), tilt angle, and analytical signal combined with upward extension methods allowed a multiscale and all round analysis of magnetic contacts. Since these methods are relatively sensitive to noise and aliasing, they require pole-reduced magnetic data. Here, the residual magnetic field data was reduced to the equator due to the strong asymmetry of magnetic anomalies observed in low magnetic latitudes (less than 45°), especially in regions close to the magnetic equator such as the Ivory Coast. This transformation has been used in many works (Baranov, 1975; Hildenbrand, 1983) in order to eliminate the distortions induced by the tilt of the Earth's magnetic field vector.

Using the above techniques, the magnetic data of the region processed show three major directional families: NW-SE, E-W, and NE-SW. These identified preferential directions have similarities with the directions of the tectonic events that affected the Ivorian Precambrian basement. These include the NE-SW birimian direction in reference to the tectonic-metamorphic deformation of the Eburnian cycle in the volcano-sedimentary formations, as well as the E-W direction of the Pan-African orogeny (Faillat, 1986). The NW-SE direction is the most marked in the basin. According to Kouamé et al. (2019), it characterises the most abundant and longest fractures mapped and uses OLI 8 satellite images in the Volta Noir basin in Côte d'Ivoire.

This study reveals that some subsurface structures have depth values. Through euler deconvolution, it is possible to delineate these contacts and evaluate their depths. The quality of this assessment depends largely on the appropriate choice of structural index (SI), which is a function of the geometry of anomalies caused by isolated and multiple anomalous sources. It also depends on the window used and the depth tolerance. The structural index or degree of homogeneity defines the type of source sought. According to Reid et al. (1990), an index between 0 and 1 should be used for mapping contacts and faults. Thompson et al. (1982) states that the correct index for a given feature is the one that provides the tightest clustering of solutions. Therefore, the SI is viewed as a primary control and

the correct SI produces the most accurate results. Since $SI=0$, characteristic of the contacts indicated satisfactory results. The new localised 3D Euler method was used instead of the standard Euler method. This is because unlike the standard Euler method, where all grid locations are tested and only those locations whose valid solutions satisfy the input criteria are retained, the localised method first calculates the grid of the analytical signal, finds the peaks in the grid, and then uses these peak locations for Euler deconvolution (Reid et al., 1990). The deep structures revealed by the Euler solutions are oriented along the N-S and NW-SE directions. These directions correspond to those of the discontinuities of the Eburnian orogeny, which is mainly N-S direction. However, this has influenced the layout of the hydrographic network of the large rivers of the Ivory Coast. In the area, it coincides with the direction of the Volta River, which is the main watercourse of the basin studied. The NW-SE direction characterises the long outcropping kilometric structures identified on the transformed magnetic images. They correlate well with the topographic fractures highlighted by the parcel studies (Youan Ta et al., 2008; Jofack-Sokeng, 2013; Mangoua, 2013; Coulibaly, 2014; Kouamé et al., 2019; Kouamé et al., 2022).

Conclusion

The use of aeromagnetic maps has revealed a network of superficial and deep structures that have affected the Precambrian basement of the Black Volta Basin in Côte d'Ivoire. These numerous lineaments representing magnetic discontinuities include fractures and faults. Quantitative analysis revealed 458 lineaments, with lengths ranging from 9.03 to 66.54 km, and a dominance, both in frequency and length, of E-W and NNE-SSW directions. Through the Euler deconvolution, it was possible to delineate some discontinuities and evaluate their depths. The estimated depths range from 6.8 to 2847 m and the deep structures are organised along N-S and NW-SE directions. These directions mark the different tectonic events that affected the Ivorian Precambrian basement. This study provides new elements on the deep structure of the study area, and thus contributes to better knowledge of the aquifer system of the Volta catchment. Subsequently, the mapping method used to identify the fracture network has proved useful. Through this means, it is possible to collect information that was previously unavailable in the region. This in turn contributes to a better understanding of the fractured reservoirs for future hydrogeological prospecting in the BVNCI. Clearly, the results obtained reveal that there is currently enough data to characterise the geometry of fractured reservoirs in the future.

Acknowledgement

The authors would like to thank the Swiss Centre for Scientific Research for the funding of project N°234/2020 between the “Programme d'Appui Stratégique à la Recherche (PASRES)” and the “Laboratoire Sciences du Sol, de l'Eau et des Géomatériaux (SSEG)” of the UFR “des Sciences de la Terre et des Ressources Minières (STRM), Abidjan, Côte d'Ivoire”.

Conflict of Interest: The authors declare no conflict of interest.

Data Availability: All of the data are included in the content of the paper.

Funding Statement: The authors did not obtain any funding for this research.

References:

1. Abbass, A. A. & Mallam, A. (2013). Estimating the Thickness of Sedimentation within Lower Benue Basin and Upper Anambra Basin, Nigeria, Using Both Spectral Depth Determination and Source Parameter Imaging. *ISRN Geophysics*.
2. Abderbi, J. & Khattach, D. (2010). The contribution of gravimetry to the study of the structure of the High Plateaux (Maroc). *Bull. Inst. Sci., Rabat, Earth Sciences section*, 32, 19-30.
3. Armel Kouame, K., Marc Youan Ta, O., Zéphir De Lasme, Derving Baka, Carine. A. M., Njeugeut Fernand, & Kouame, K. (2019). Analysis of Fracture Networks of the Black Volta Catchment in Côte D'ivoire; *Journal of Geography, Environment and Earth Science International (JGEESI) ISSN: 2454-7352, n°46635, Feb. 2019, 1-14p*
4. Asfirane-haddadj, F. & Galdeano, A. (2000). The use of Euler deconvolution and analytical signal for locating magnetic sources. *Bulletin of the Geological Society, France*, (1), 71-81.
5. Baranov, V. (1957). A new method for interpretation of aeromagnetic maps: pseudo gravimetric anomalies. *Geophysics*, 22 (2), 359-382.
6. Bouiflane, M. (2008). Aeromagnetic and magnetic multi-scale mapping: structural study of a region of the Rhine Graben. *Thèse de Doctorat, Université Louis Pasteur, Strasbourg 1*.
7. Coulibaly, A. (2014). Contribution of the electrical resistivity method (Trails and Electrical Soundings) to the location of aquifers in crystalline and crystallophyllous basement zones: the case of the Tanda region (north-east of Côte d'Ivoire), PhD thesis, Félix Houphouët Boigny University 148 p
8. El Gout, R., Khattach, D., Houari, M. R., Kaufmann, O., & Aqil, H. (2010). Main structural lineaments of northeastern Morocco derived

- from gravity and aeromagnetic data. *Journal of African Earth Science*, (58), 255–271.
9. Faillat, J. P. (1985). Fissured aquifers in humid tropical zones: structure, hydrodynamics and hydrochemistry (West Africa). University thesis. Languedoc (Montpellier), 534 p.
 10. Grauch, V. J. S., Sawyer, D. A., Minor, S. A., Hudson, M. R., & Thompson, R. A. (2006). Gravity and Aeromagnetic Studies of the Santo Domingo Basin Area, New Mexico. Chapter D of *The Cerrillos Uplift, the La Bajada Constriction and Hydrogeologic Framework of the Santo Domingo Basin, Rio Grande Rift, New Mexico*, edited by Scott A. Minor. U. S. Geological Survey, Denver, 63-86.
 11. Jofack-Sokeng, V.C. (2013). Contributions of neural networks to the lithostructural mapping of the Precambrian basement of the Bondoukou region (north-east of Côte d'Ivoire), Earth Sciences MASTER degree dissertation. University. Félix Houphouët BOIGNY (Abidjan), 94 p
 12. Keating, P. (1997). Automated trend reinforcement of aeromagnetic data. *Geophysical Prospecting*, 45 (3), 521-534.
 13. Khattach, D., Keating, P., Mili, E., Chennouf, T., Andrieux, P., & Milhi, A. (2004). The contribution of gravimetry to the study of the structure of the Triffa cathment (north-eastern Morocco): hydrogeological implications. *Comptes Rendus Géoscience*, (336), 1427-1432.
 14. Lachassagne, P. & Wyns, R. (2005). Aquifères de socle : nouveaux concepts - Application à la prospection et la gestion de la ressource en eau. *Géosciences* 2, p. 32-37.
 15. Mangoua, J. (2013). Evaluation of the potential and vulnerability of the groundwater resources of the fissured aquifers of the Baya catchment area (East of Côte d'Ivoire). PhD thesis, 171p. Nanguy Abrogoua University.
 16. Miller, H.G. & Singh, V. (1994). Potential field tilt- a new concept for location of potential field sources. *Journal of applied Geophysics*, 32, 213-217.
 17. Ousmane, B. (1988). Etude géochimique et isotopique des aquifères du socle de la bande sahélienne du Niger (Liptako, Sud-Maradi et Zinder-Est). Thèse Univ. Niamey. 175 p. *Journal of African Earth Science*, (58), 255–271.
 18. Reeves, C. (2005). Aeromagnetic surveys: principles, practice and interpretation. Course unit i, 50, 150 pages.
 19. Reid, A. B., Allsop, J. M., Granser, H., Millett, A. J., & Somerton, I.W. (1990). Magnetic interpretation in three dimensions using Euler deconvolution. *Geophysics*, 55, 80-91.

20. Salem, A., William, S., Fairhead, D., Smith, R., & Ravat, D. (2008). Interpretation of magnetic data using tilt-angle derivatives. *Geophysics*, 73, NO. 1 _JANUARY-FEBRUARY 2; P. L1–L10, 7 FIGS.
21. Vanié, L.T.A., Khattach, D., & Houari, M. R., (2005). Contribution of gravity anomaly filtering to the study of deep structures in eastern Morocco. *Bulletin of the Scientific Institute, Rabat, Earth Sciences section*, (27), 29-40.
22. Verduzco, B., Fairhead, J. D., Green, C. M., & Mackenzie, C. (2004). New insights into magnetic derivatives for structural mapping. *SEG the Leading Edge February*, 116-119.
23. Youan Ta, M., Lasm, T., Jourda, J. P., Kouame. K. F., & Razack, M. (2008). Structural mapping using Landsat-7 ETM+ satellite imagery and analysis of fracture networks in the Precambrian basement of the Bondoukou region (north-eastern Côte d'Ivoire). *Remote Sensing Journal*, 2008, vol. 8, no. 2, p. 119-135, 2008, vol. 8, n° 2, p. 119-135.